

Article

## Two Dimensional Temperature Distributions in Plate Heat Exchangers: An Analytical Approach

Amir Reza Ansari Dezfoli, Mozaffar Ali Mehrabian \* and Mohamad Hasan Saffaripour

Department of Mechanical Engineering, Shahid Bahonar University of Kerman, P.O. Box 76175-133, Kerman 76135-133, Iran; E-Mails: kadr\_basteh@yahoo.com (A.R.A.D.); m.h.saffaripour@mail.uk.ac.ir (M.H.S.)

\* Author to whom correspondence should be addressed; E-Mail: ma\_mehrabian@alum.mit.edu; Tel.: +98-3422111763.

Academic Editor: Palle E. T. Jorgensen

Received: 20 June 2015 / Accepted: 30 November 2015 / Published: 16 December 2015

---

**Abstract:** Analytical solutions are developed to work out the two-dimensional (2D) temperature changes of flow in the passages of a plate heat exchanger in parallel flow and counter flow arrangements. Two different flow regimes, namely, the plug flow and the turbulent flow are considered. The mathematical formulation of problems coupled at boundary conditions are presented, the solution procedure is then obtained as a special case of the two region Sturm-Liouville problem. The results obtained for two different flow regimes are then compared with experimental results and with each other. The agreement between the analytical and experimental results is an indication of the accuracy of solution method.

**Keywords:** plate heat exchanger; temperature distribution; analytical approach; Sturm-Liouville problem

---

### 1. Introduction

The study of the coupled forms of heat transfer between forced convection flows and conduction in surfaces is very important due to the existence of these simultaneous effects in practical heat transfer processes. In particular, the design and performance of counter flow multilayered heat exchangers offer excellent opportunities to analyze these complex physical phenomena. Many theoretical investigations of heat transfer characteristics of heat exchangers under plug, laminar, and turbulent flows have been

published in the literature. Specifically, research on fin efficiency, double pipe, and parallel plate exchangers is progressing. In connection with the conjugate heat transfer process over surfaces, the effect of wall heat conduction and convective heat transfer has been analyzed in several works.

The temperature distribution in a horizontal flat plate of finite thickness was analyzed by Luikov [1] and Payvar [2]. In this conjugate problem the lower surface was maintained at a uniform temperature, while the upper surface was transferring heat to a laminar boundary layer by convection. Two approximate solutions were presented by Luikov [1], based respectively on differential and integral analyses. The first solution was performed considering low Prandtl number assumption, while the second solution was conducted using polynomial forms for the velocity and temperature profiles. In the case of large Prandtl numbers the Lighthill approximation [3] was used by Payvar [2] and an integral equation was obtained and then solved numerically.

From the practical point of view, the specific wall temperature boundary condition is the least important, since its use as a representation of an actual condition in a plate heat exchanger is applicable only for certain special limiting cases. Boundary conditions that specify heat fluxes apply more directly to any actual situation, such as coolant passages of nuclear reactors.

Except for certain special circumstances, none of the boundary conditions treated in the literature would be applicable. In view of the practical importance of heat exchangers in general, it is surprising that investigations of applicable Sturm-Liouville problem have not been investigated. A possible reason for this appears to be related to the applicability of the classical mathematical techniques to obtain analytical solutions to similar problems. However, the analytical treatment of Graetz and conjugated Graetz problems is mainly based on the Eigen-function expansion technique in terms of power series in many studies [4]. Nunge and Gill [5] developed an orthogonal expansion technique for solving a new class of counter-flow heat transfer problems. Nunge and Gill [5] solved the exchanger problem assuming fully developed laminar velocity profiles, negligible conduction in the fluid streams, and temperature independent fluid properties.

The main purpose of this paper is conducting an introductory analytical investigation of temperature distribution in parallel flow and counter flow plate heat exchangers using Sturm-Liouville problem. Mehrabian [6] derived one dimensional temperature distributions in plate heat exchangers using four simplifying assumptions. These assumptions were uniform heat flux, constant overall heat transfer coefficient, linear relationship between the overall heat transfer coefficient and cold flow temperature, linear relationship between the overall heat transfer coefficient and temperature difference between cold and hot flows. Ansari *et al.* [7] developed a mathematical model to analyze the heat transfer characteristics in a double pipe heat exchanger. They used laminar flow assumption for flow in the internal tube and turbulent flow in the annular channel in parallel flow arrangement. The heat transfer coefficients derived for inner flow and outer flow were predicted using the mathematical model and compared with standard correlations. The model deviation from the standard correlation was less than 10 percent [7]. This paper is an extension of [6,7], using analytical approach to obtain temperature distributions in plate heat exchangers in longitudinal direction as well as in the direction perpendicular to the plates.

The temperature distribution in plate heat exchangers is obtained based on a two region Sturm-Liouville system consisting of two equations coupled at common boundary. The solutions of this system form an infinite sequence of Eigen functions with corresponding eigenvalues. If the velocity distributions are

assumed to be uniform, the Eigen functions are the familiar tabulated functions and eigenvalues are given by the positive nonzero roots of an eigenvalue transcendental equation. The plug flow and the turbulent flow models of the heat exchanger fluid flows are utilized in this paper with the following idealizations:

- 1- At the inlet to each channel the temperature is uniform in the channel cross-section.
- 2- Frictional heating is negligible.
- 3- Longitudinal heat conduction in the plates is negligible.
- 4- Physical properties are temperature independent.
- 5- Longitudinal heat conduction in the fluids is negligible.
- 6- The effect of corrugations in flow and heat transfer is neglected.

The first three idealizations are reasonable in most heat exchangers applications. The fourth idealization is normally acceptable when considering density, specific heat and thermal conductivity for liquid-liquid applications. The variations of viscosity with respect to temperature in plate heat exchanger channels were studied by Mehrabian *et al.* [8]. Their study shows, in a plate heat exchanger with water as the process and service fluid the performance does not considerably change when an average viscosity based on  $T = (T_{inlet} + T_{outlet})/2$  is used for each fluid. The accuracy of this assumption is more pronounced when  $T_{in} - T_{out}$  is not very large.

The fifth idealization has been shown to be valid for a variety of special cases when Peclet numbers are larger than 50 [9–11], it seems reasonable to assume that this idealization is valid for the particular cases of interest here, where Peclet number exceeds 50. The sixth idealization can be more realistic by considering the developed plate area instead of the projected plate area in heat transfer calculations.

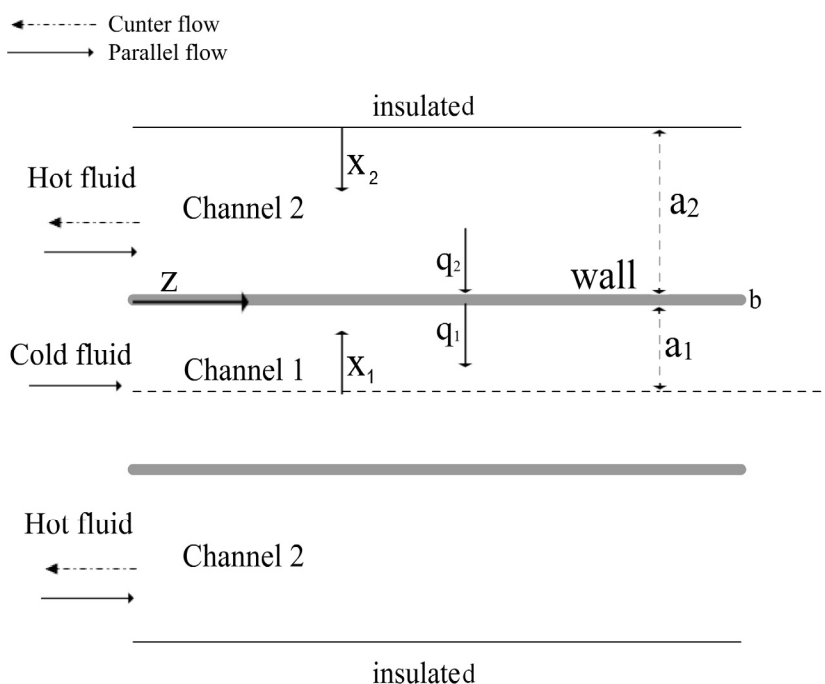


Figure 1. Plate heat exchanger geometry.

## 2. Problem Description and Mathematical Formulation Based on Plug Flow Model

The plate heat exchanger consists of channels separated by common walls with fluids flowing through the channels, as illustrated in Figure 1. Plate heat exchangers are widely used, their great advantage being their diversity of application and simplicity of construction. They consist of a number of rectangular plates separated with gaskets to contain a constant space and then clamped together. The gaskets control the inlet and outlet ports in the corners of the plates, allowing the hot and cold fluids to flow in alternative channels of the exchanger. Since it is easy to alter the number of plates used in an exchanger, and since a wide variety of flow arrangements is possible, these exchangers can be used for many applications [6].

Based on the previous simplifications, the energy conservation and Fourier’s heat conduction law, for the heat exchanger channels shown in Figure 1 are as follows:

$$u_1 \frac{\partial T_1}{\partial z} = \alpha_1 \frac{\partial^2 T_1}{\partial x_1^2} \tag{1}$$

$$(-1)^m u_2 \frac{\partial T_2}{\partial z} = \alpha_2 \frac{\partial^2 T_2}{\partial x_2^2} \tag{2}$$

where  $\alpha = \frac{k}{\rho c}$ ,  $m = 0$  for parallel flow,  $m = 1$  for counter flow,  $u_1$  and  $u_2$  are the absolute values of velocity. The symmetry and wall boundary conditions are:

$$x_i = 0: \frac{\partial T_i}{\partial x_i} = 0 \tag{3}$$

$$x_i = a_i: q_1 - q_2 = 0 \Rightarrow k_1 \frac{\partial T_1}{\partial x_1} + k_2 \frac{\partial T_2}{\partial x_2} = 0 \tag{4}$$

Heat balance equation at the interface of fluid 1 and wall ( $x_1 = a_1$ ) can be expressed as;

$$q_1 = q_w \Rightarrow k_1 \frac{\partial T_1}{\partial x_1} = k_w \frac{T_2(a_2, z) - T_1(a_1, z)}{b} \tag{5}$$

Equations (1) and (2) are special cases of the two-region Sturm-Liouville problem.

### 2.1. Dimensionless Equations

The dimensionless space variables for channel 1 and 2 are respectively defined as follows:

$$X_1 = \frac{x_1}{a_1} \tag{6}$$

$$X_2 = \frac{x_2}{a_2} \tag{7}$$

The dimensionless length  $Z$  is defined for channels 1 and 2, referenced arbitrarily to the properties of channel 1:

$$Z = \frac{4}{Pe_1} \left( \frac{z}{2a_1} \right) \tag{8}$$

where  $Pe_1$  is the Peclet number for channel 1, defined as:

$$Pe_1 = \frac{2a_1u_1}{\alpha_1} \tag{9}$$

Other dimensionless parameters are defined as follows:

$$H = \frac{c_2\dot{M}_2}{c_1\dot{M}_1} \tag{10}$$

$$K = \frac{k_1a_2}{k_2a_1} \tag{11}$$

$$K_w = \frac{k_1b}{k_wa_1} = \frac{\frac{k_1}{a_1}}{\frac{k_w}{b}} = \frac{R_1^{-1}}{R_w^{-1}} = \frac{R_w}{R_1} \tag{12}$$

$$\psi^2 = KH \tag{13}$$

$$\theta_i(X_i, Z) = \frac{T_i - T_{c(Z=0)}}{T_{h(Z=0)} - T_{c(Z=0)}} \tag{14}$$

The governing equations and boundary condition are re-written in terms of dimensionless variables  $\theta_i$ ,  $X_i$  and  $Z$ :

$$\frac{\partial^2\theta_1}{\partial X_1^2} = \frac{\partial\theta_1}{\partial Z} \tag{15}$$

$$\frac{\partial^2\theta_2}{\partial X_2^2} = (-1)^m \psi^2 \frac{\partial\theta_2}{\partial Z} \tag{16}$$

$$\theta_1(X_1, 0) = 0 \tag{17}$$

$$\theta_2(X_2, 0) = 1 \tag{18}$$

$$X_i = 0: \frac{\partial\theta_i}{\partial X_i} = 0 \tag{19}$$

$$X_i = 1: K \frac{\partial\theta_1}{\partial X_1} + \frac{\partial\theta_2}{\partial X_2} = 0 \tag{20}$$

$$X_i = 1: K_w \frac{\partial\theta_1}{\partial X_1} + \theta_1(1, Z) - \theta_2(1, Z) = 0 \tag{21}$$

### 2.2. Solution

To solve the problem, the method of separation of variables is used. A separation in the following form is assumed for channel 1:

$$\theta_1(X_1, Z) = N_1(Z) \cdot M_1(X_1) \tag{22}$$

Applying Equation (22) to Equation (15) gives:

$$\frac{M_1''(X_1)}{M_1(X_1)} = \frac{N_1'(Z)}{N_1(Z)} = k = -\lambda_n^2 \tag{23}$$

where  $\lambda$  is the Eigen value. Equation (22) will become indeterminate for positive  $k$  while for negative  $k$ ,  $\theta_1$  will converge to a limiting value, this is explained with more details in [4,5,12]. The solution for  $N_1(Z)$  with respect to  $\lambda$  is:

$$N_1(Z) = e^{-\lambda_n^2 Z} \tag{24}$$

Thus

$$\theta_1(X_1, Z) = \sum_{n=0}^{\infty} C_n M_{1n}(X_1) e^{-\lambda_n^2 Z} \tag{25}$$

A similar method applied to Equation (17) gives:

$$\theta_2(X_2, Z) = \sum_{n=0}^{\infty} C_n M_{2n}(X_2) e^{-\lambda_n^2 Z} \tag{26}$$

Applying the new variables  $\theta_1$  and  $\theta_2$  into Equation (15) and Equation (16) yields:

$$M_{1n}''(X_1) + \lambda_n^2 M_{1n}(X_1) = 0 \tag{27}$$

$$M_{2n}''(X_2) + (-1)^m \cdot \psi^2 \lambda_n^2 M_{2n}(X_2) = 0 \tag{28}$$

Applying the new variables  $\theta_1$  and  $\theta_2$  into Equation (20) to Equation (22) gives:

$$M_{1n}'(0) = 0 \tag{29}$$

$$M_{2n}'(0) = 0 \tag{30}$$

$$K \cdot M_{1n}'(1) + M_{2n}'(1) = 0 \tag{31}$$

$$K_w \cdot M_{1n}'(1) + M_{1n}(1) - M_{2n}(1) = 0 \tag{32}$$

### 2.3. Eigenvalue Equation

Assuming  $M_{1n}(X_1) = A \cdot F(\lambda, X_1)$  and  $M_{2n}(X_2) = B \cdot G(\lambda, X_2)$ , where  $A$  and  $B$  are arbitrary constants, for  $\lambda = \lambda_0, \lambda_1, \lambda_2, \lambda_3, \dots$ , Equation (31) and Equation (32) respectively become:

$$K A F'_{X_1}(\lambda, 1) + B G'_{X_2}(\lambda, 1) = 0 \tag{33}$$

$$A [K_w F'_{X_1}(\lambda, 1) + F(\lambda, 1)] - B G(\lambda, 1) = 0 \tag{34}$$

We can write Equations (33) and (34) as:

$$\begin{bmatrix} K F'_{X_1}(\lambda, 1) & G'_{X_2}(\lambda, 1) \\ K_w F'_{X_1}(\lambda, 1) + F(\lambda, 1) & -G(\lambda, 1) \end{bmatrix} \begin{bmatrix} A \\ B \end{bmatrix} = \begin{bmatrix} 0 \\ 0 \end{bmatrix}$$

In order this system of simultaneous homogeneous linear algebraic equations have nonzero solutions for  $A$  and  $B$ , the coefficient determinant must be made equal to zero by proper choice of  $\lambda$ :

$$\begin{bmatrix} KF'_{X_1}(\lambda, 1) & G'_{X_2}(\lambda, 1) \\ K_w F'_{X_1}(\lambda, 1) + F(\lambda, 1) & -G(\lambda, 1) \end{bmatrix} = 0$$

This gives the eigenvalue equation:

$$F(\lambda, 1)G'_{X_2}(\lambda, 1) + KF'_{X_1}(\lambda, 1)G(\lambda, 1) + K_w F'_{X_1}(\lambda, 1)G'_{X_2}(\lambda, 1) = 0 \tag{35}$$

In order to find  $\lambda = \lambda_0, \lambda_1, \lambda_2, \lambda_3, \dots$  for each condition (K, Kw, H), Equation (35) should be solved.  $S(\lambda)$  represents Equation (35) for parallel flow and counter flow conditions in Table 1.

**Table 1.** F, G and Eigen functions for parallel flow and counter flow plate heat exchangers.

Type	$F(\lambda, X_1)$	$G(\lambda, X_2)$	$S(\lambda)$
Parallel flow	$\cos(\lambda X_1)$	$\cos(\psi \lambda X_2)$	$\cos(\lambda) \sin(\psi \lambda) + \frac{K}{\psi} \sin(\lambda) \cos(\psi \lambda) - K_w \lambda$ $\sin(\lambda) \sin(\psi \lambda) = 0$
Counter flow	$\cos(\lambda X_1)$	$\cosh(\psi \lambda X_2)$	$\cos(\lambda) \sinh(\psi \lambda) - \frac{K}{\psi} \sin(\lambda) \cosh(\psi \lambda) - K_w \lambda$ $\sin(\lambda) \sinh(\psi \lambda) = 0$

For  $K = 1, H = 1, K_w = 0$  we have following Eigenvalues (parallel flow condition):

$$\lambda = \lambda_0, \lambda_1, \lambda_2, \lambda_3, \lambda_4, \lambda_5 \dots$$

$$\lambda = 1.5705, 3.1415, 4.7125, 6.2835, 7.8535, 9.4245 \dots$$

and for  $K = 1, H = 1, K_w = 0$  we have following Eigenvalues (Counter flow condition):

$$\lambda = \lambda_0, \lambda_1, \lambda_2, \lambda_3, \lambda_4, \lambda_5 \dots$$

$$\lambda = 3.9266, 7.0686, 10.2102, 13.3518, 16.4934, 19.6350 \dots$$

Equation (33) gives:

$$B = -K \frac{F'_{X_1}(\lambda, 1)}{G'_{X_2}(\lambda, 1)} A \tag{36}$$

Since the system is homogeneous, either  $A$  or  $B$  can be chosen arbitrarily, Hence:

$$A = G_{X_2}(\lambda, 1) \tag{37}$$

The Eigen functions  $M_{1n}$  and  $M_{2n}$  can be represented by:

$$M_{1n}(X_1) = AF(\lambda, X_1) = G_{X_2}(\lambda, 1)F(\lambda, X_1) \tag{38}$$

$$M_{2n}(X_2) = BG(\lambda, X_2) = -KF_{X_1}(\lambda, 1)G(\lambda, X_2) \tag{39}$$

Constants  $A$  and  $B$  calculated in this section satisfy Equation (34). Ansari [13] proved that for arbitrary constants  $\psi$ ,  $K$ ,  $K_w$ , and values of  $A$ , and  $B$  obtained in this section Equation (34) is true. He [13] also calculated the values of  $\lambda$  for which the boundary conditions are fulfilled.

2.4. Finding  $F(\lambda, X_1)$  and  $G(\lambda, X_2)$

The solution for Equation (27) along with boundary condition, Equation (20) is:

$$M_{1n}(X_1) = AF(\lambda, X_1) = A \cos(\lambda X_1) \tag{40}$$

Equation (28) and boundary condition for channel 2 are:

$$M_{2n}''(X_2) + (-1)^m \psi^2 \lambda^2 M_{2n}(X_2) = 0 \tag{41}$$

$$M_{2n}'(0) = 0 \tag{42}$$

The solution for counter flow arrangement ( $m = 1$ ) is:

$$M_{2n}(X_2) = BG(\lambda, X_2) = B \cosh(\psi \lambda X_2) \tag{43}$$

$F(\lambda, X_1)$ ,  $G(\lambda, X_2)$  and Eigen functions are given in Table 1 for plate heat exchangers.  $M_{1n}(X_1)$  and  $M_{2n}(X_2)$  are also given in Equations (38) and (39).

2.5. Orthogonality of the Eigen functions

The orthogonality condition for the  $M_{1n}$  and  $M_{2n}$  will now be established. The differential Equation (27) is first manipulated for  $n = i$  and  $j$  in the same manner used to derive properties of the familiar Sturm-liouville system. For example, Equation (27) is written for  $n = i$  and then for  $n = j$  with  $i \neq j$ . the equation for  $n = i$  is multiplied by  $M_{1j}$  and the equation for  $n = j$  is multiplied by  $M_{1i}$ . The two resulting equations are subtracted, simplified and then integrated between  $X_1 = 0$  and  $X_1 = 1$ . The following equation is obtained:

$$(\lambda_j^2 - \lambda_i^2) \int_0^1 M_{1j}(X_1)M_{1i}(X_1)dX_1 = M_{1j}(1)M_{1i}'(1) - M_{1i}(1)M_{1j}'(1) \tag{44}$$

In a similar manner, Equation (28) is written for  $n = i$  and then for  $n = j$  with  $i \neq j$ . the equation for  $n = i$  is multiplied by  $M_{2j}$  and the equation for  $n = j$  is multiplied by  $M_{2i}$ . The two resulting equations are subtracted, simplified and then integrated between  $X_2 = 0$  and  $X_2 = 1$ . The following equation is obtained;

$$\psi^2 (\lambda_j^2 - \lambda_i^2) \int_0^1 M_{2j}(X_2)M_{2i}(X_2)dX_2 = M_{2j}(1)M_{2i}'(1) - M_{2i}(1)M_{2j}'(1) \tag{45}$$

Equations (44) and (45) can be related to each other using the coupling boundary conditions at  $X = 1$ . Thus, Equations (31) and (32) respectively become:

$$M_{2n}'(1) = -KM_{1n}'(1) \tag{46}$$

$$M_{2n}(1) = M_{1n}(1) + K_w M_{1n}'(1) \tag{47}$$

Using these conditions in Equations (44) and (45) gives:

$$\int_0^1 M_{1i}(X_1)M_{1j}(X_1)dX_1 + \int_0^1 HM_{2j}(X_2)M_{2i}(X_2)dX_2 = 0 \quad i \neq j \tag{48}$$

Equation (48) is the orthogonality condition for the Eigen function  $M_{1n}$  and  $M_{2n}$ . For the case of  $i = j = n$ , Equation (48) leads to a normalizing factor defined by:

$$N_n = \int_0^1 M_{1n}^2(X_1)dX_1 + \int_0^1 HM_{2n}^2(X_2)dX_2 \tag{49}$$

Equations (38) and (39) for the case of  $n = 0$  with  $\lambda = 0$  give

$$M_{10} = M_{20} = 1$$

Applying the above condition into Equation (49) gives:

$$N_0 = 1 + H \tag{50}$$

### 2.6. Finding $C_n$ and $\theta_i$

The following expansions are considered regarding Equations (25) and (26) at  $Z = 0$ :

$$0 = \sum_{n=0}^{\infty} C_n M_{1n}(X_1) \tag{51}$$

$$1 = \sum_{n=0}^{\infty} C_n M_{2n}(X_2) \tag{52}$$

Multiplying Equation (51) by  $M_{1n}(X_1)dX_1$  and Equation (52) by  $H.M_{2n}(X_2)dX_2$ , adding the resulting expressions and integrating between  $X_i = 0$  and  $X_i = 1$  using Equation (49), the following equation for the  $C_n$  is obtained:

$$C_n = \frac{1}{N_n} \int_0^1 HM_{2n}(X_2)dX_2 \tag{53}$$

Equations (50) and (53) give:

$$C_0 = \frac{H}{N_0} = \frac{H}{1 + H} \tag{54}$$

Using Equations (38), (39) and (53) and simplifying the results gives:

$$A_{1n} = C_n.M_{1n}(X_1) = \frac{2G_{X_2}(\lambda, 1)F(\lambda, X_1)}{\psi\lambda^2.S'(\lambda)} \tag{55}$$

$$A_{2n} = C_n.M_{2n}(X_2) = (-1)^{l-m} \cdot \frac{2KF_{X_1}(\lambda, 1).G(\lambda, X_2)}{\psi\lambda^2.S'(\lambda)} \tag{56}$$

where  $S'(\lambda)$  is the differential of the Eigen function. The solution for the two-dimensional temperature distribution can subsequently be written as:

$$\theta_i(X_i, Z) = \frac{H}{1+H} + \sum_{n=1}^{\infty} A_{in}(X_i).e^{-\lambda_n^2.Z} \tag{57}$$

The average temperature can be used as one-dimensional form of temperature distribution:

$$\theta_{Bi}(X_i) = \int_0^1 \theta_i(X_i, Z) dX_i = \frac{H}{1+H} + \int_0^1 \left( \sum_{n=1}^{\infty} A_{in}(X_i).e^{-\lambda_n.Z} \right) dX_i \tag{58}$$

### 3. Modification for the Turbulent Flow

Equations (1) and (2) used for plug flow condition in Section 2 can be applied for turbulent flow when  $\alpha$  is replaced by  $\alpha + \varepsilon$  [14]. Since  $\alpha = k/\rho c$ , the general form for Equations (1) and (2) applied to turbulent flow becomes:

$$\frac{\partial}{\partial X} \left[ (k + c\rho\varepsilon) \frac{\partial T}{\partial X} \right] = c\rho u \frac{\partial T}{\partial Z} \tag{59}$$

In this equation  $\varepsilon$  represents a turbulent diffusivity for heat transfer. The term  $k + c\rho\varepsilon$  can be interpreted as an effective total conductivity,  $k_t$  written as:

$$k_t = k \left( 1 + \frac{\varepsilon}{\nu} Pr \right) \tag{60}$$

where  $\nu$  is the kinematic viscosity and  $Pr$  is the Prandtl number. Now an average effective conductivity  $k_m$  is defined:

$$k_m = \int_0^1 k_t dX \tag{61}$$

The  $k_m$  value for the parallel plate channel was obtained experimentally by Lyon [15], He proposed the following correlation for predicting  $k_m$  with respect to Peclet number:

$$k_m = \frac{k}{6} (5.8 + 0.02Pe^{0.8}) \tag{62}$$

The average effective conductivity,  $k_m$ , must be applied to Equations (11) and (12) in order to convert the plug flow solution into the turbulent flow solution. In other words,  $K$  in Equation (11) and  $K_w$  in Equation (12) are respectively replaced by:

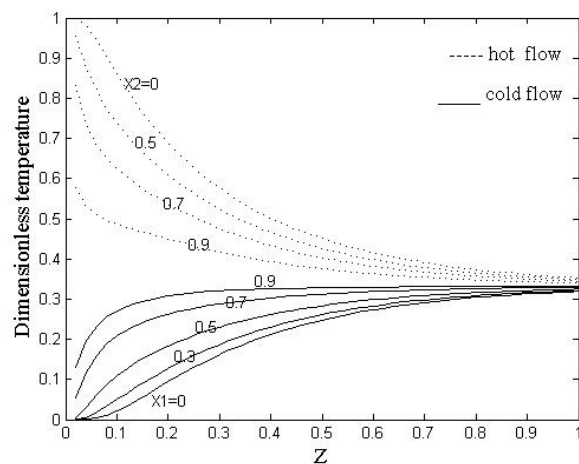
$$K_t = \left( \frac{k_{m1}a_2}{k_{m2}a_1} \right) \tag{63}$$

and

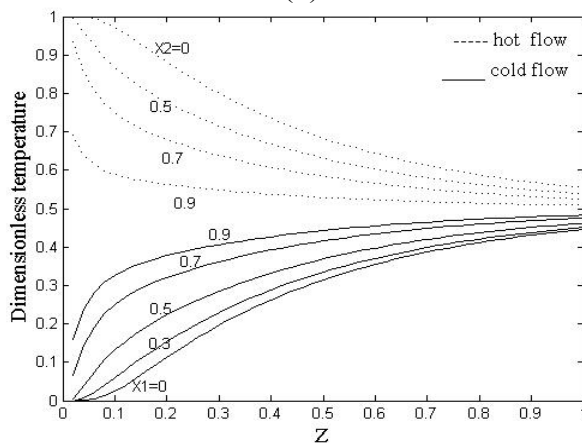
$$K_{wt} = \left( \frac{k_{m1}b}{k_w a_1} \right) \tag{64}$$

4. Results

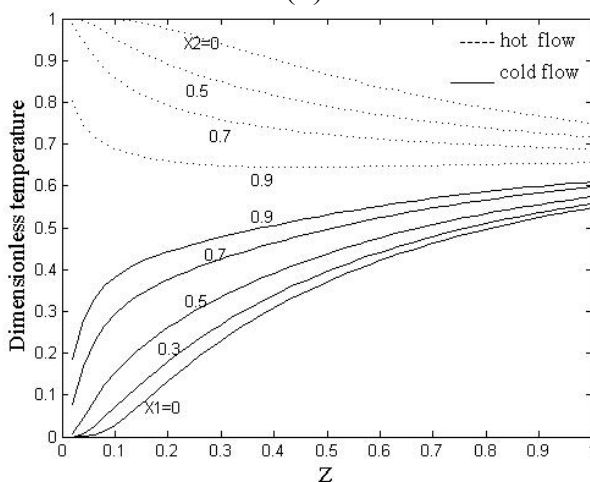
The results are presented in four different cases representing in Figures 2–5.



(a)

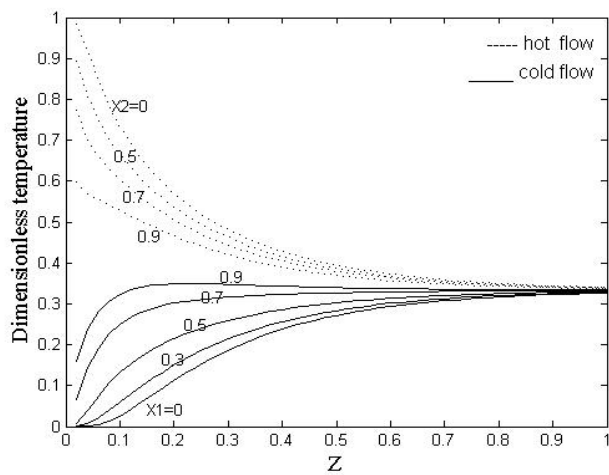


(b)

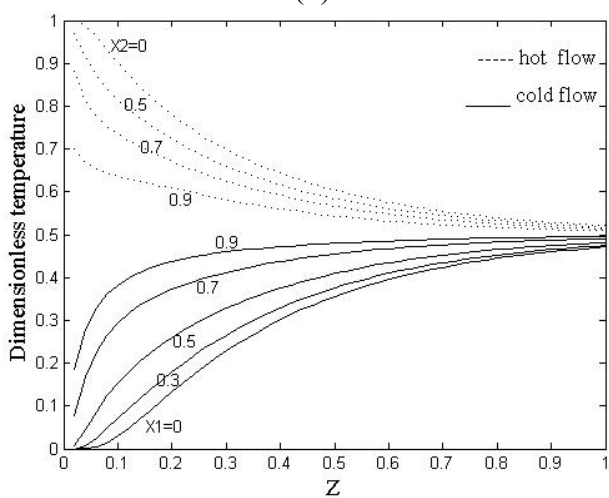


(c)

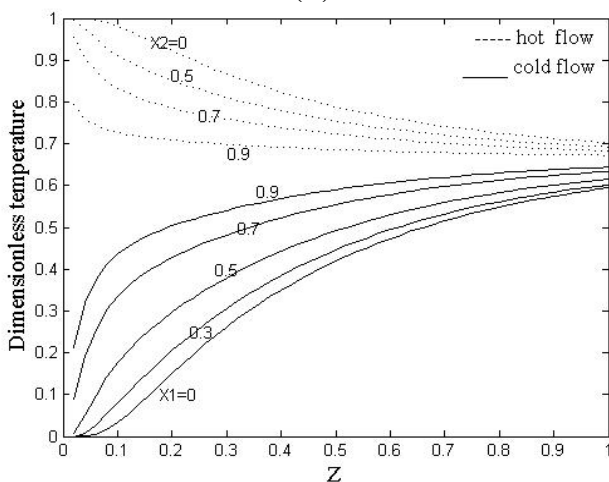
**Figure 2.** Temperature distribution for a parallel flow plate heat exchanger (Plug flow). (a) Two dimensional temperature distribution for  $K = 1$ ,  $H = 0.5$ ,  $K_w = 0$ ; (b) Two dimensional temperature distribution for  $K = 1$ ,  $H = 1$ ,  $K_w = 0$ ; (c) Two dimensional temperature distribution for  $K = 1$ ,  $H = 2$ ,  $K_w = 0$ .



(a)

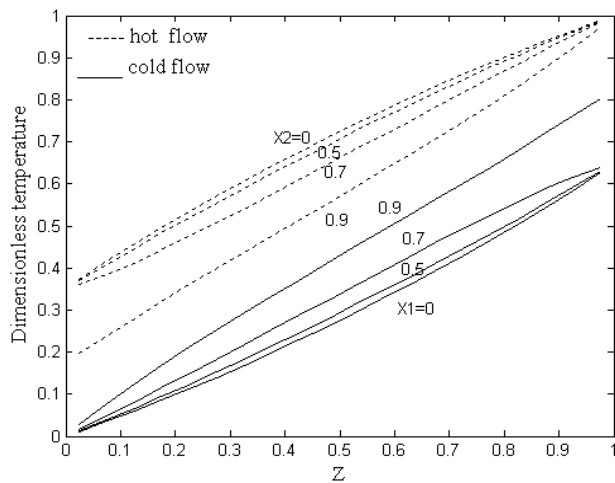


(b)

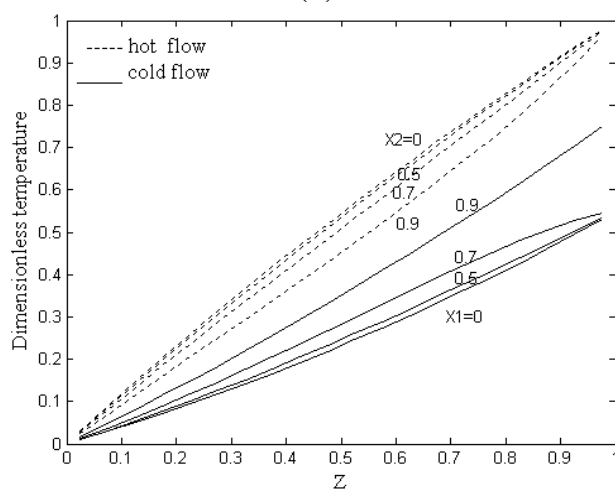


(c)

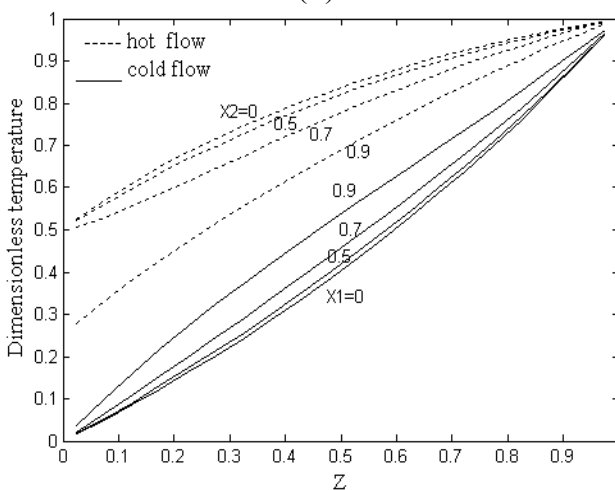
**Figure 3.** Temperature distribution for a parallel flow plate heat exchanger (Turbulent flow).  
 (a) Two dimensional temperature distribution for  $K = 1$ ,  $H = 0.5$ ,  $K_w = 0$ , and  $K_t = 0.33$ ;  
 (b) Two dimensional temperature distribution for  $K = 1$ ,  $H = 1$ ,  $K_w = 0$  and  $K_t = 0.33$ ;  
 (c) Two dimensional temperature distribution for  $K = 1$ ,  $H = 2$ ,  $K_w = 0$  and  $K_t = 0.33$ .



(a)

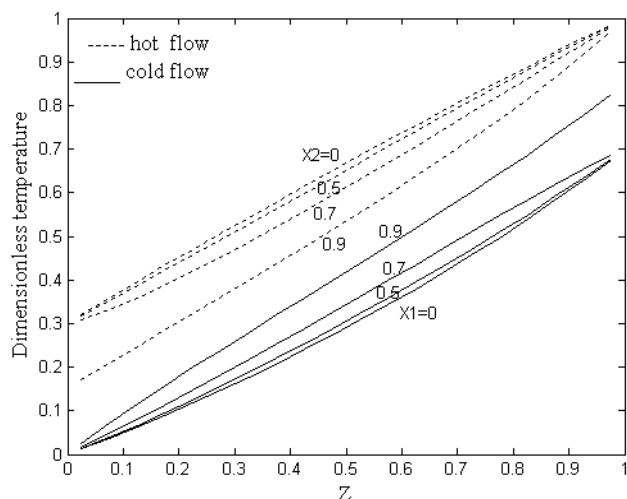


(b)

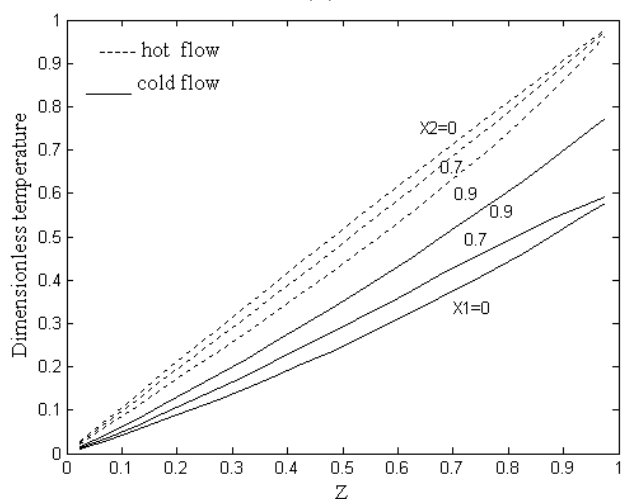


(c)

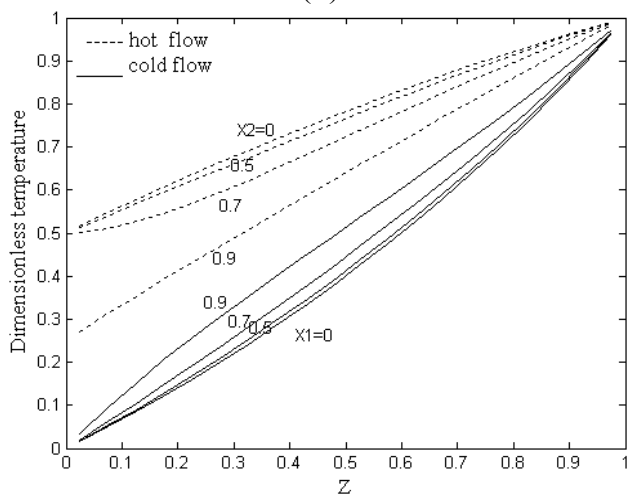
**Figure 4.** Temperature distribution for a counter flow plate heat exchanger (Plug flow). (a) Two dimensional temperature distribution for  $K = 1$ ,  $H = 0.5$ ,  $K_w = 0$ ; (b) Two dimensional temperature distribution for  $K = 1$ ,  $H = 1$ ,  $K_w = 0$ ; (c) Two dimensional temperature distribution for  $K = 1$ ,  $H = 2$ ,  $K_w = 0$ .



(a)



(b)



(c)

**Figure 5.** Temperature distribution for a counter flow plate heat exchanger (Turbulent flow).  
 (a) Two dimensional temperature distribution for  $K = 1$ ,  $H = 0.5$ ,  $K_w = 0$  and  $K_t = 0.33$ ;  
 (b) Two dimensional temperature distribution for  $K = 1$ ,  $H = 1$ ,  $K_w = 0$ , and  $K_t = 0.33$ ;  
 (c) Two dimensional temperature distribution for  $K = 1$ ,  $H = 2$ ,  $K_w = 0$  and  $K_t = 0.33$ .

4.1. Parallel Flow Arrangement-Plug Flow Regime ( $Pe_1 = 75000$ , and  $Pe_2 = 3500$ )

The dimensionless temperature distributions for hot and cold flows in this case are shown in Figure 2 for  $K_w = 0$ , where  $K_w$  is defined in Equation (12), the wall thermal resistance ( $R_w$ ) is much smaller than the fluid thermal resistance ( $R_w \ll R_1$ ), therefore  $K_w$  is very small ( $K_w \approx 0$ ).

4.2. Parallel Flow Arrangement-Turbulent Flow Regime ( $Pe_1 = 75000$ , and  $Pe_2 = 3500$ )

The dimensionless temperature distributions for hot and cold flows in this case are shown in Figure 3 for  $K_w = 0$  and  $K_t = 0.33$ .

4.3. Counter Flow Arrangement-Plug Flow Regime ( $Pe_1 = 75000$ , and  $Pe_2 = 3500$ )

The dimensionless temperature distributions for hot and cold flows in this case are shown in Figure 4 for  $K_w = 0$ .

4.4. Counter Flow Arrangement-Turbulent Flow Regime ( $Pe_1 = 75000$ , and  $Pe_2 = 3500$ )

The dimensionless temperature distributions for hot and cold flows in this case are shown in Figure 5 for  $K_w = 0$  and  $K_t = 0.33$ .

5. Comparison, Validation, and Discussion

The temperature distribution obtained for counter flow arrangement is compared with the established experimental data available in the literature using similar plate dimensions and flow details [6,16,17]. To get a clearer picture of the problem, a plate heat exchanger consisting of four standard plates is considered. Plate dimensions and flow details are shown in Table 2. Fluid temperatures at five intermediate points in the main chevron region are evaluated.

Table 2. Plate dimensions and flow details.

Developed Plate Length	$L$	1 m
Flow wide	$W$	0.35 m
Flow thickness	$2a_1, a_2$	0.00367 m
Wall thickness	$b$	0.0006 m
Thermal conductivity of wall	$k_w$	73 W/m.K
	Hot fluid	Cold fluid
Inlet temperature	77.9 °C	47.9 °C
Outlet temperature	71.7 °C	76.9 °C
Heat capacity	4191J/kg.K	4184 J/kg.K
Mass flow rate	472.6 kg/h	101.2 kg/h
density	994 kg/m <sup>3</sup>	994 kg/m <sup>3</sup>
Kinematics Viscosity × 10 <sup>6</sup>	0.461 m <sup>2</sup> /s	0.623 m <sup>2</sup> /s
Thermal conductivity	0.664 W/m.K	0.651 W/m.K
Pr	3.48	3.75
Re	406.8	64.4

The plate dimensions briefly mentioned in Table 2 correspond to standard APV SR3 chevron plates, which are widely used in the process industry [16]. The flow details given in Table 2 have been applied in a test machine. The local temperatures along the central exchanger channel (cold fluid flow) have been measured experimentally [16].

The dimensionless parameters for analytical procedure are as follows:

$$H = 4.68, K_t = 1.03, K_{t,w} = 0.0015, \psi^2 = 4.59 \tag{65}$$

The experimental data [15] and analytical-numerical results developed in [6] are listed in Table 3. In reality, the temperature varies not only along z, but also along x. Table 3 is dedicated to the variations of temperature along z.

**Table 3.** Temperature distribution of the cold flow in two sides of the central channel of the plate heat exchanger.

$T_E$ (°C)	$T_N$ (°C)	Error	$T$ (°C)	Error	Distance
47.9	47.9	0	47.9	0	0 m
61.9	60.3	2.6	62.6	3.1	1/6 m
66.8	67.6	1.2	66.1	0.4	2/6 m
70.2	72	2.6	69.7	1.5	3/6 m
72.6	74.5	2.6	72.1	2	4/6 m
74.3	76	2.2	74.6	1.8	5/6 m
76.9	76.9	0	76.9	0	1 m

$T_E$ : Experimental data [14],  $T_N$ : Local temperature of plate heat exchanger using the analytical-numerical method developed in [15] for constant overall heat transfer coefficient,  $T$ : Local temperature of plate heat exchanger using the analytical method developed in this paper.

Mehrabian *et al.* [17] established an experimental technique to measure the local temperatures along the flow channels of a plate heat exchanger. Mehrabian, *et al.* [18] also conducted a three dimensional computational analysis to investigate the hydrodynamics and thermal characteristics of plate heat exchangers. In this investigation they predicted the temperature, pressure, and velocity distributions in the flow channels of a plate heat exchanger. The present paper tackles the same problem from an analytical point of view, and therefore completes this cycle of computational, experimental, and analytical methodologies. Each methodology has its own difficulties, analytical approach however requires the governing equations are as simplified as possible and this leads to certain simplifying assumptions. The major assumptions affecting the analytical results are:

- Ignoring the heat transfer enhancement in the development region for the fluids,
  - Not taking account of the effect of corrugations by assuming the plates are flat, and
  - Assuming turbulent flow in the flow channels while the Reynolds numbers are not large enough.
- It should be mentioned that the flow visualization experiments [19] support this assumption.

## 6. Conclusions

In this study, the mathematical model of the heat transfer phenomena in a plate heat exchanger with counter flow or parallel flow arrangements has been developed and investigated. The analytical

solution is obtained based on a two region Sturm-Liouville system consisting of two equations coupled at a common boundary. In order to provide mathematical simplicity, a plug flow model of the heat exchanging fluids were utilized for this analysis. An approximate method was developed for converting the plug flow formulation into the turbulent flow formulation. The mathematical method performed in this study can be applied for the prediction of the temperature distribution. The predictions of the method developed in this study are in close agreement with experimental results available in the literature.

### Acknowledgments

The corresponding author would like to express his deep gratitude to the reviewers for their time and valuable suggestions. They carefully reviewed the paper three times and gave instructions to improve the scientific content of the paper.

### Author Contributions

This paper is extradcted from the MSc thesis of the first author supervised by the second author.

### Conflicts of Interest

The authors declare no conflict of interest.

### Nomenclature

#### Dimensional Quantities

$2a_1$	Width of channel 1, m
$a_2$	Width of channel 2, m
$b$	Wall thickness, m
$k_i$	Thermal conductivity of fluid i, W/m.K
$k_w$	Thermal conductivity of wall. W/m.K
$k_t$	Thermal conductivity for turbulent flow, W/m.K
$k_m$	Average effective conductivity, W/m.K
$\alpha_i$	Thermal diffusivity of fluid i, m <sup>2</sup> /s
$c_i$	Heat capacity of fluid i, J/kg.K
$q_i$	Heat flux density at wall in channel i, W/m <sup>2</sup>
$T_i$	Local temperature of fluid i, °C
$T_{c(in)}$	Inlet temperature for channel 1, °C
$T_{h(in)}$	Inlet temperature for channel 2, °C
$T_{h(out)}$	Outlet temperature for channel 2, °C
$x$	Coordinate normal to heat transfer surface, m
$z$	Axial coordinate or heat exchanger length, m
$u_i$	Absolute value of the velocity of fluid i
$\nu$	Kinematic viscosity, m <sup>2</sup> /s
$\varepsilon$	Turbulent diffusivity for heat transfer, m <sup>2</sup> /s

$W$  Plate wide, m

$\lambda$  Eigenvalue

#### Dimensionless Quantities

$H$	Heat capacity flow rate ratio
$K$	Relative thermal resistance of fluid
$K_w$	Relative thermal resistance of wall
$Pe$	Peclet number
$Pr$	Prandtl number
$Re$	Reynolds number
$\theta_i$	Local temperature of fluid i
$X$	Dimensionless distances
$Z$	Dimensionless length
$\dot{M}$	Mass flow rate of fluid, kg/s

#### SUBSCRIPTS

$B$	Average temperature
$c$	Cold
$h$	Hot
$m$	0 for parallel flow , 1 for counter flow
$n$	0, 1, 2, 3, ...
$t$	Turbulent

## References

1. Luikov, A.V. Conjugate convective heat transfer problems. *Int. J. Heat Mass Transf.* **1974**, *17*, 257–265.
2. Payvar, P. Convective heat transfer to laminar flow over a plate of finite thickness. *Int. J. Heat Mass Transf.* **1977**, *20*, 431–433.
3. Lighthill, M.J. Contributions to the theory of heat transfer through a laminar boundary layer. *Proc. R. Soc. A* **1950**, *202*, 359–377.
4. Yeh, H.M.; Ho, C.D. The improvement of performance in parallel plate heat exchangers by inserting in parallel an impermeable sheet for double-pass operations. *Chem. Eng. Commun.* **2000**, *183*, 39–48.
5. Nunge, R.J. Gill, W.N. An analytical study of laminar counterflow double pipe heat exchangers. *AIChE J.* **1966**, *12*, 279–289.
6. Mehrabian, M.A. Longitudinal temperature changes in plate heat exchanger: Analytical-numerical approach. *Iran. J. Sci. Technol.* **2003**, *27*, 573–588.
7. Ansari, A.R.; Mehrabian, M.A. The overall heat transfer characteristics of a double pipe heat exchanger. In Proceedings of the National Conference of Mechanical Engineering, Tehran, Iran, 10–12 May 2008.
8. Mehrabian, M.A.; Khoramabadi, M. Application of numerical methods to study the effect of variable fluid viscosity on the performance of plate heat exchangers. *Int. J. Numer. Methods Heat Fluid Flow* **2007**, *17*, 94–107.
9. Mehrabian, M.A.; Sheikhzadeh, G.A.; Khoramabadi, M. Application of numerical methods to study the effect of axial conduction in plates and flow channels on the performance of plate heat exchangers. *Int. J. Numer. Methods Heat Fluid Flow* **2006**, *16*, 67–83.
10. Eckert, E.R.; Drake, R.M. *Heat and Mass Transfer*; McGraw-Hill: New York, NY, USA, 1959; pp. 298–301.
11. Poppendiek, H.F. Turbulent Liquid-Metal Heat Transfer in Channels. *Nucl. Sci. Eng.* **1959**, *5*, 390–398.
12. Mikhailov, M.D.; Ozisik, M.N. *Unified Analysis and Solutions of Heat and Mass Diffusion*; John Wiley and Sons: Hoboken, NJ, USA, 1984; p. 55.
13. Ansari, A.R. Study of Thermal Characteristics of Double Pipe and Plate Heat Exchangers Using the Exact Solution of Sturm-Liouville Equation in One and Two Dimensional Cases. Master's Thesis, Shahid Bahonar University of Kerman, Kerman, Iran, 2008.
14. Kays, W.M.; Crawford, M.E. *Convective Heat and Mass Transfer*; McGraw-Hill: New York, NY, USA, 1966.
15. Lyon, R. Liquid metal heat transfer coefficients. *Chem. Eng. Prog.* **1951**, *47*, 47–75.
16. Hasler, L.E.; *et al.* Flow Distribution in a Plate and Frame Heat Exchanger. In Proceedings of the 3rd UK National Heat Transfer Conference, Birmingham, UK, 16–18 September 1992; Volume 1, pp. 361–367.
17. Mehrabian, M.A.; Poulter, R. Hydrodynamics and thermal characteristics of corrugated channels: Computational approach. *Appl. Math. Model.* **2000**, *24*, 343–364.

18. Mehrabian, M.A.; Poultr, R.; Quarini, G.L. Hydrodynamic and thermal characteristics of corrugated channels: Experimental approach. *Exp. Heat Transf.* **2000**, *13*, 223–234.
19. Vlasogiannis, P.; Karagiannis, G.; Argyropoulos, P.; Bontozoglou, V. Air-water two-phase flow and heat transfer in a plate heat exchanger. *Int. J. Multiph. Flow* **2002**, *28*, 757–772.

© 2015 by the authors; licensee MDPI, Basel, Switzerland. This article is an open access article distributed under the terms and conditions of the Creative Commons Attribution license (<http://creativecommons.org/licenses/by/4.0/>).